

Viscoelasticity of Copolymers and Polymer Blends with Bicontinuous and Other Structures

M. Takahashi

Kyoto Institute of Technology, Japan

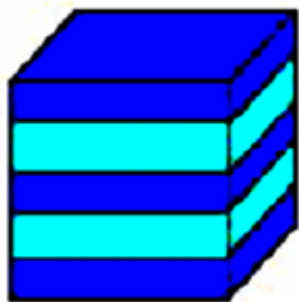
Part I

Structure and Rheology of Block and Starblock Copolymers

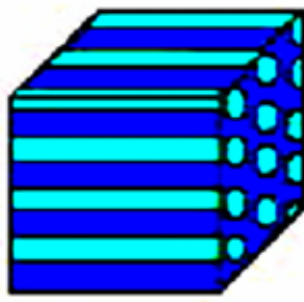
Objectives

For SB block and starblock copolymers, to clarify

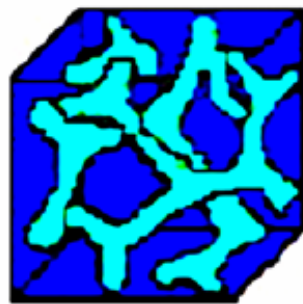
1. Structure-rheology relationships for lamellar-, cylinder- and **gyroid**-forming samples
2. Flow-induced orientations by large amplitude oscillatory shear (**LAOS**) and steady flow (SF)



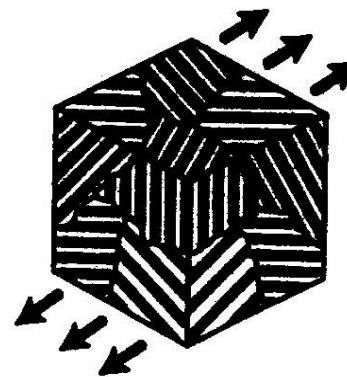
Lamella



Cylinder

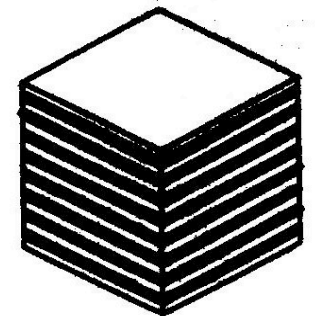


Gyroid



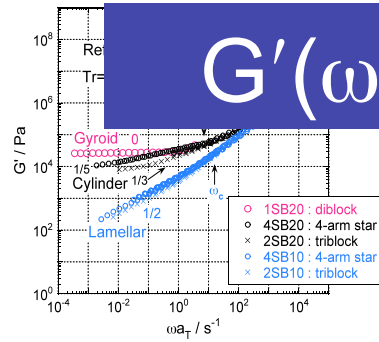
Poly-grain

LAOS



orientation

$G'(\omega)$ of SB Block Copolymers



chain
motion

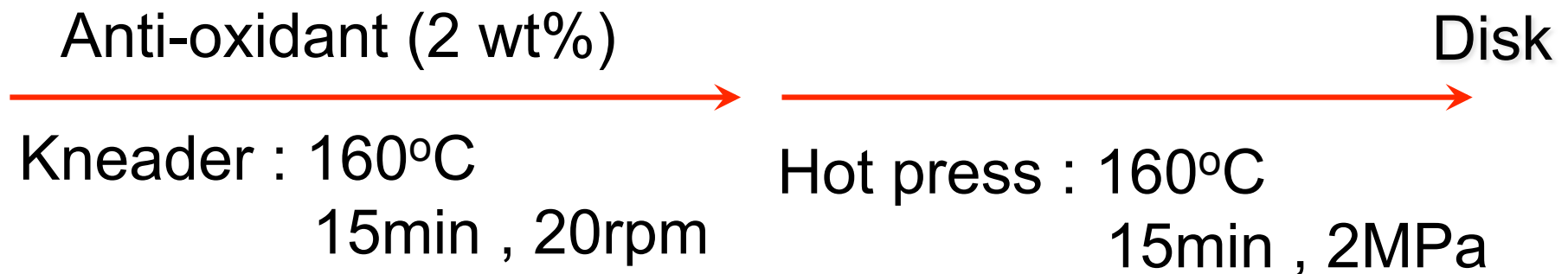
defects and
grain
boundary

motion of lamellar,
cylinder, and gyroid
domains

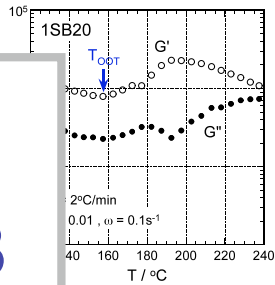
Gyroid-Forming
SB Diblock Copolymer

SB Diblock Copolymer

Code	$M_n(S)$	$M_n(B)$	f(B)	M_w/M_n
1SB20	20.1K	10.8K	0.36	1.09



Temperature Sweep of G' and G''



Cylinder

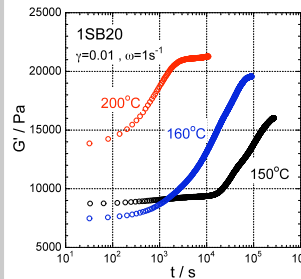
Gyroid

Time Sweep of G' for 1SB20

20K 10K
S  B

$T_{OOT} \approx 160^{\circ}\text{C}$

G' becomes stable
after 74 hr at 150°C
after 25 hr at 160°C
after 40 min at 200°C



Ⓒ
↓

Gyroid

Ⓓ

Cylinder

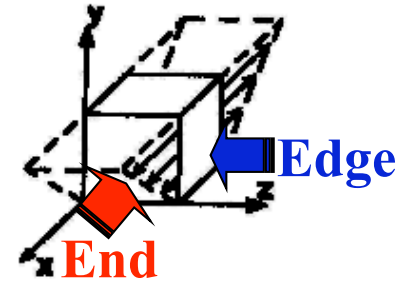
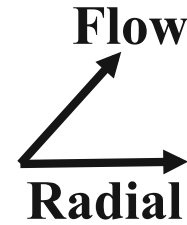
Ⓐ

TEM Micrographs of 1SB20

Cylinder

(A)

Initial State



End



Flow



Radial

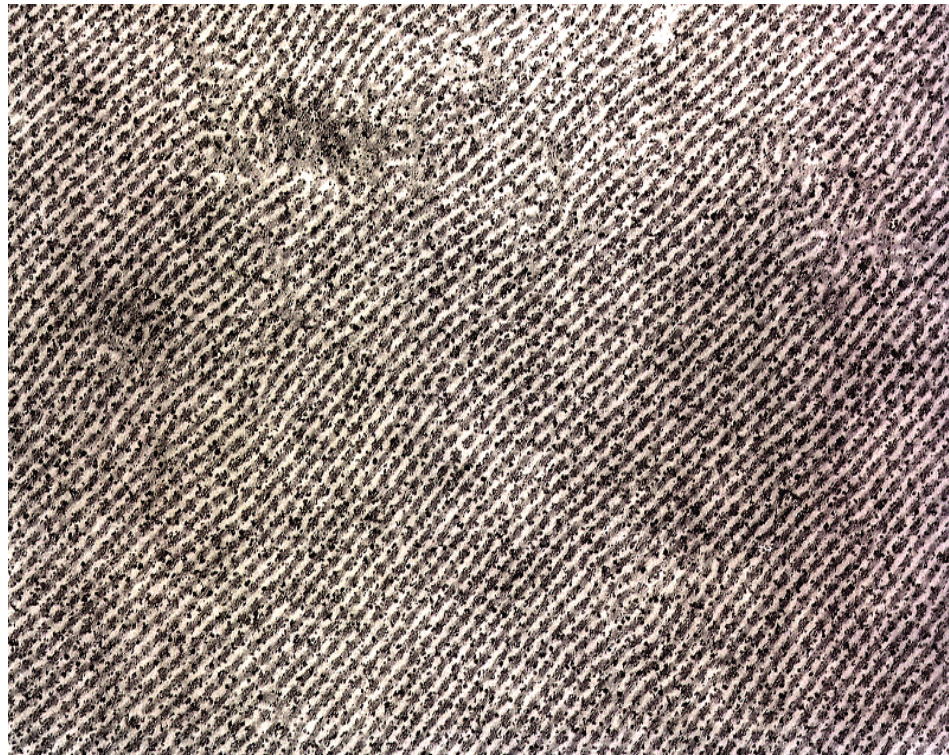
Edge



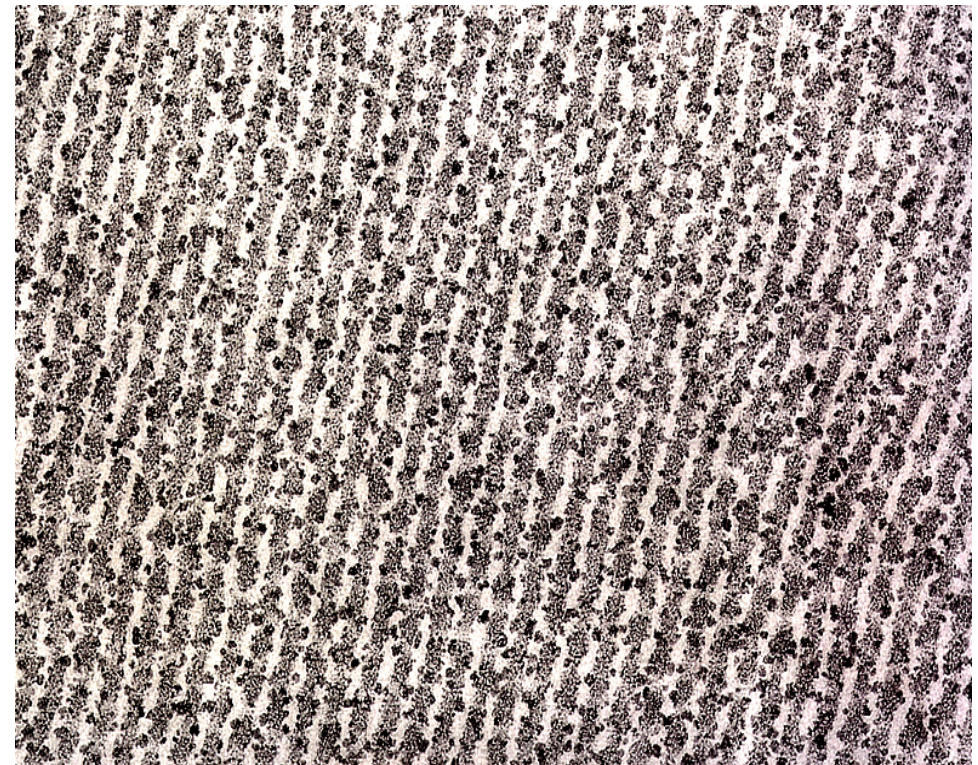
Radial



Flow



100nm



50nm

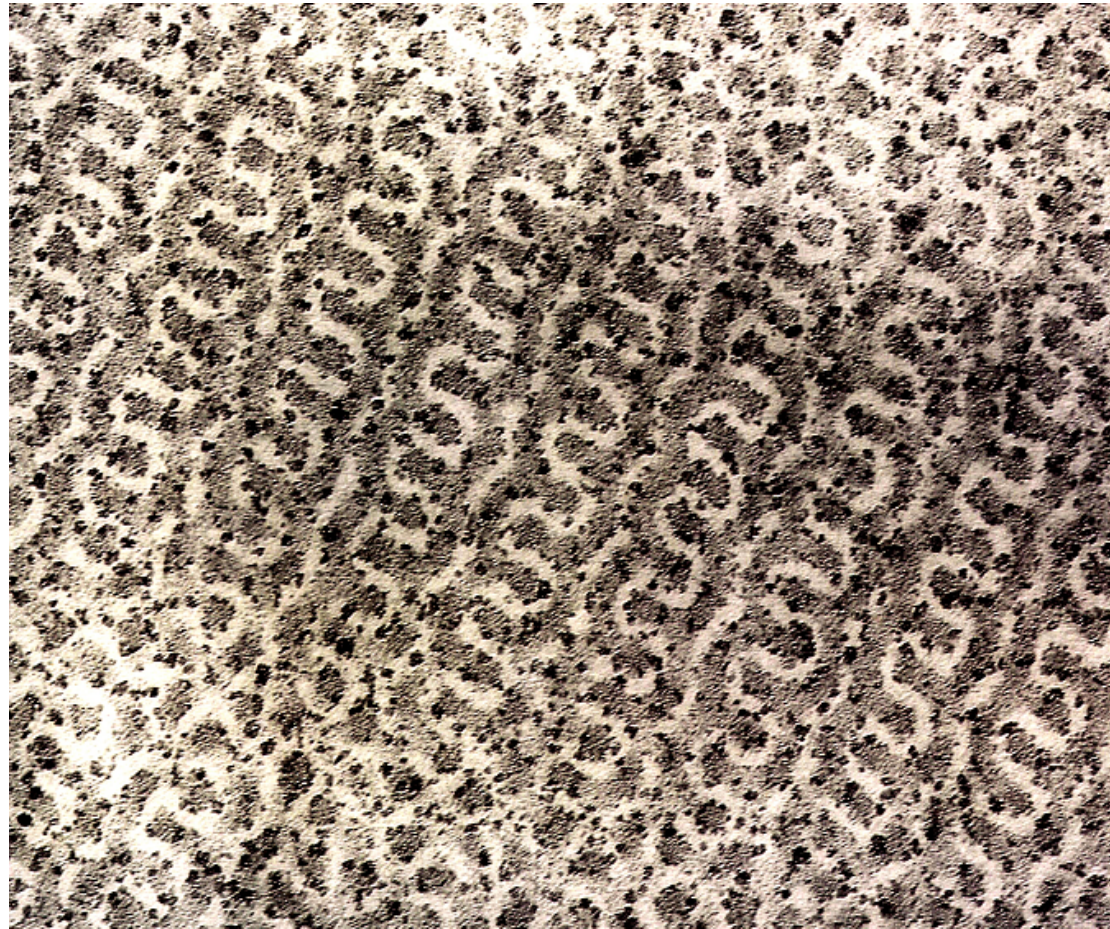
Quenched from $T=160^{\circ}\text{C}$ after Stabilization

(B)

Edge

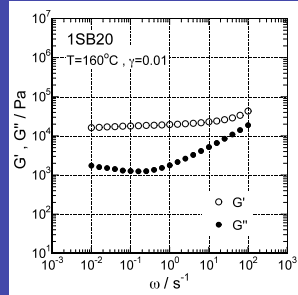
⊙ Radial → Flow

Gyroid



50nm

G' and G'' at T=160°C after Stabilization



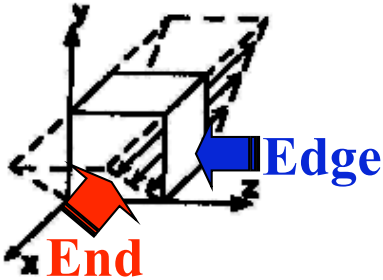
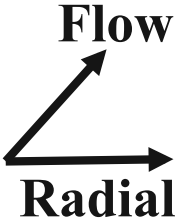
ⓑ

$$G_{\text{cubic}} = 1.85 \times 10^4 \text{ Pa}$$



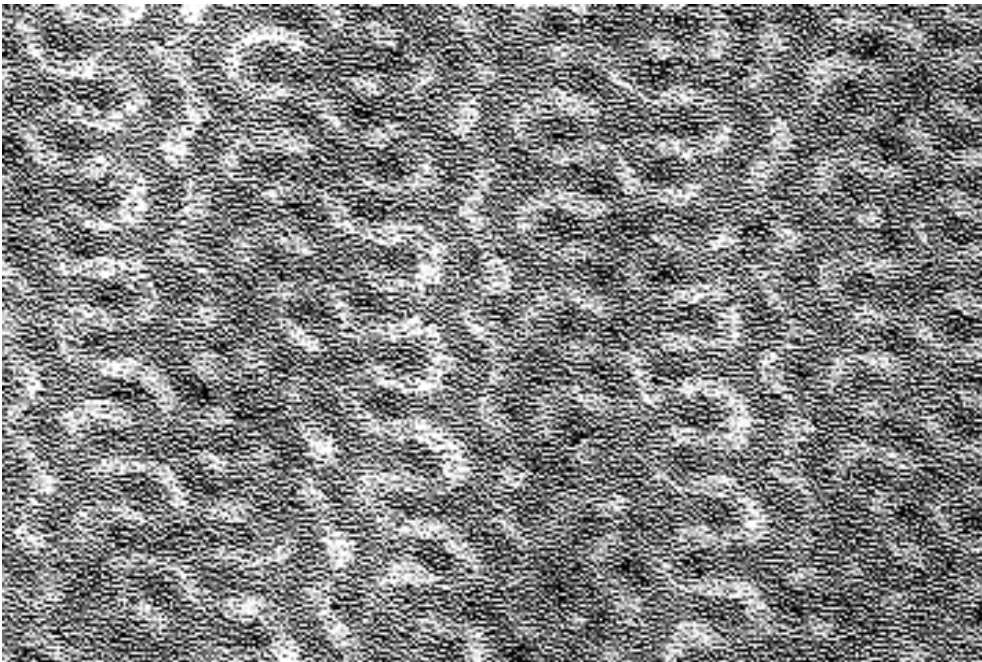
Quenched from $T=200^{\circ}\text{C}$ after Stabilization

Gyroid



End

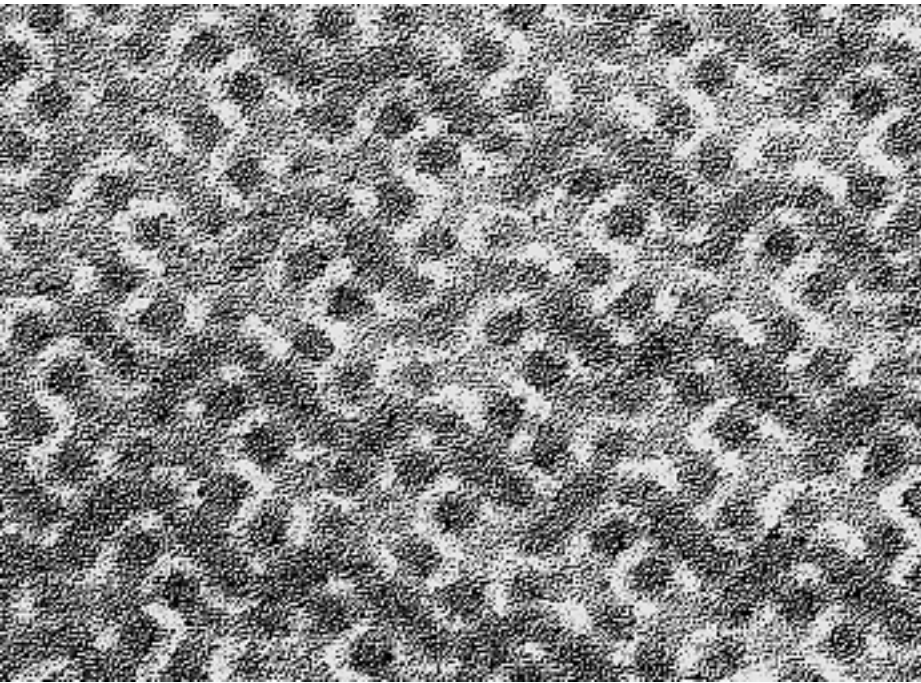
⊙ **Flow**



50nm

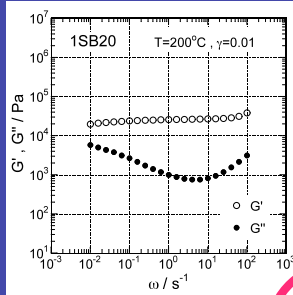
Edge

⊙ **Radial**



50nm

G' and G'' at T=200°C after stabilization

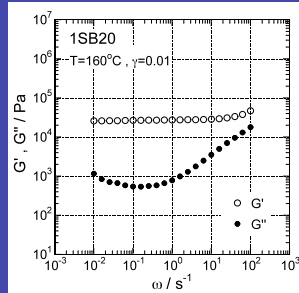


©

$$G_{\text{cubic}} = 2.61 \times 10^4 \text{ Pa}$$



G' and G'' at T=160°C after stabilized at T=200°C



200°C → 160°C

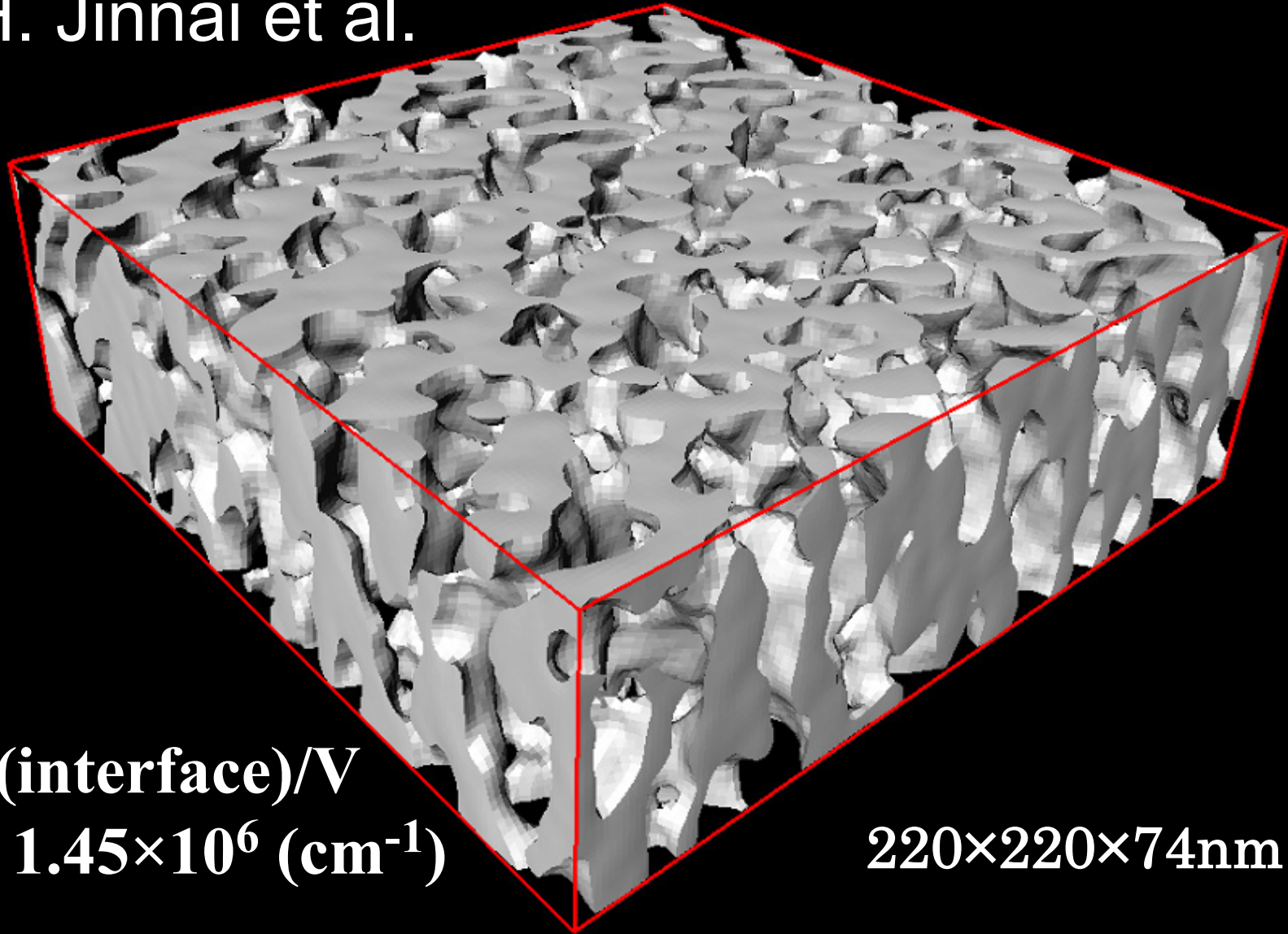
$$G_{\text{cubic}} = 2.71 \times 10^4 \text{ Pa}$$



3D TEM Image of 1SB20

(quenched from 160°C after stabilization at 200°C)

H. Jinnai et al.

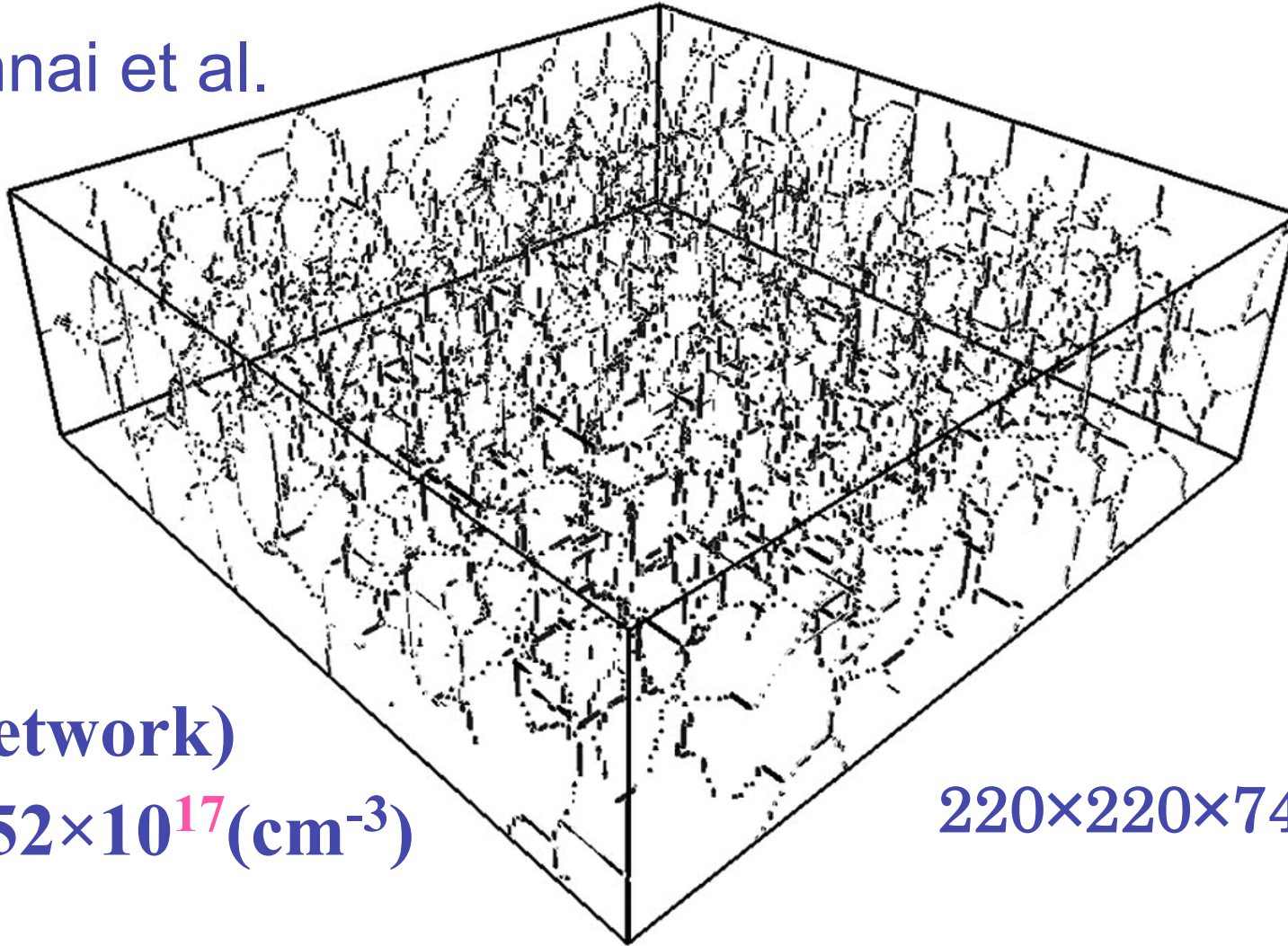


$$\frac{S(\text{interface})}{V} = 1.45 \times 10^6 \text{ (cm}^{-1}\text{)}$$

220×220×74nm

Result of 3D Thinnig for 1SB20 (quenched from 160°C after stabilization at 200°C)

H. Jinnai et al.



$v(\text{network})$
 $= 3.52 \times 10^{17} (\text{cm}^{-3})$

$220 \times 220 \times 74 \text{nm}$

3-branch: 75% average length: 15.3nm

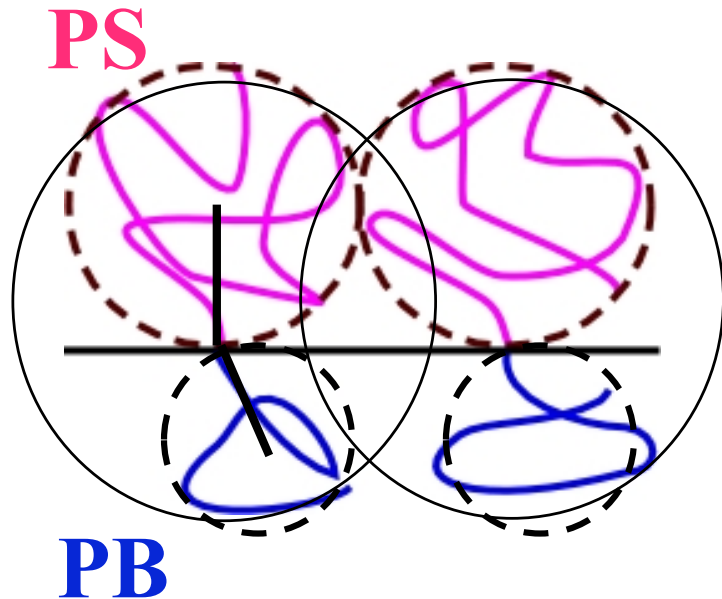
$$G_{\text{cubic}} = \nu kT$$

ν : # of molecules per unit volume

$$\nu(G_{\text{cubic}}) = 4.58 \times 10^{18} \text{ (cm}^{-3}\text{)}$$

$$\nu(\text{network}) = 3.52 \times 10^{17} \text{ (cm}^{-3}\text{)}$$

$$\nu(\text{interface}) = \frac{S(\text{interface}) / V}{S(\text{per chain})} = 3.63 \times 10^{18} \text{ (cm}^{-3}\text{)}$$



$$S(\text{interface}) / V = 1.45 \times 10^6 \text{ (cm}^{-1}\text{)}$$

$$S(\text{per chain}) = \pi \langle S^2 \rangle$$

$$\langle S^2 \rangle = \frac{1}{6} [(C_{\infty} N l^2)_{\text{PS}} + (C_{\infty} N l^2)_{\text{PB}}]$$

$$G_{\text{cubic}} = \nu kT$$

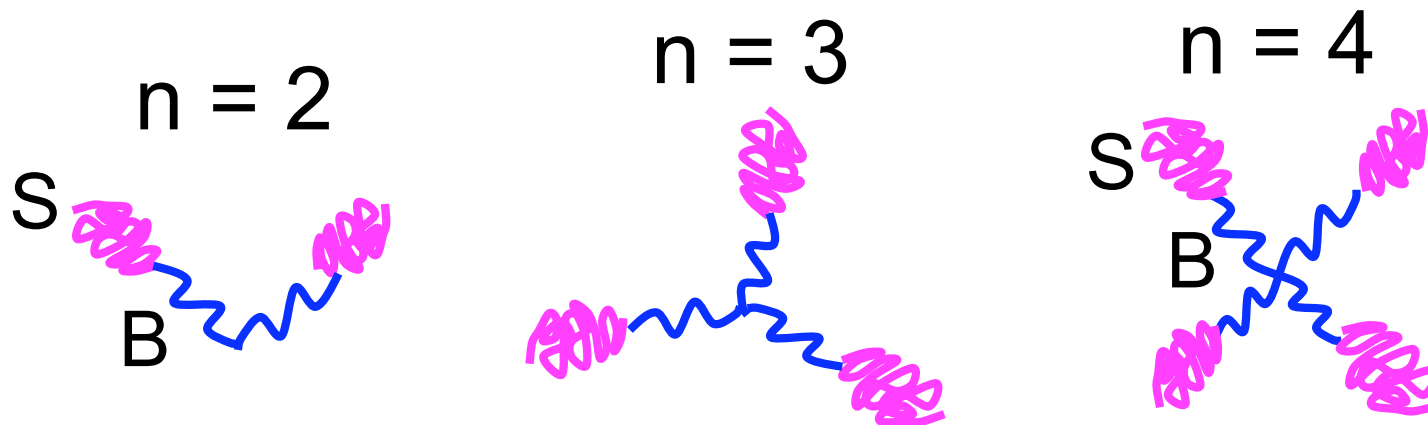
ν : # of molecules per unit volume

	160°C after stabilized at 200°C	stabilized at 200°C (C)	stabilized at 160°C (B)
$\nu(G_{\text{cubic}})$ (cm ⁻³)	4.58×10^{18}	4.00×10^{18}	3.10×10^{18}
$\nu(\text{network})$ (cm ⁻³)	3.52×10^{17}	3.28×10^{17}	2.20×10^{17}
$\nu(\text{interface})$ (cm ⁻³)	3.63×10^{18}	2.78×10^{18}	3.36×10^{18}

Lamellar-Forming
SB Starblock Copolymer

(SB)_n Star Block Copolymers

n	Code	Arm		f _{PB}	L
		M _n (PS)	M _n (PB)		
2	2SB10	9.31K	11.6K	0.56	L
3	3SB10	9.53K	11.4K	0.55	L
4	4SB10	9.51K	11.4K	0.55	L

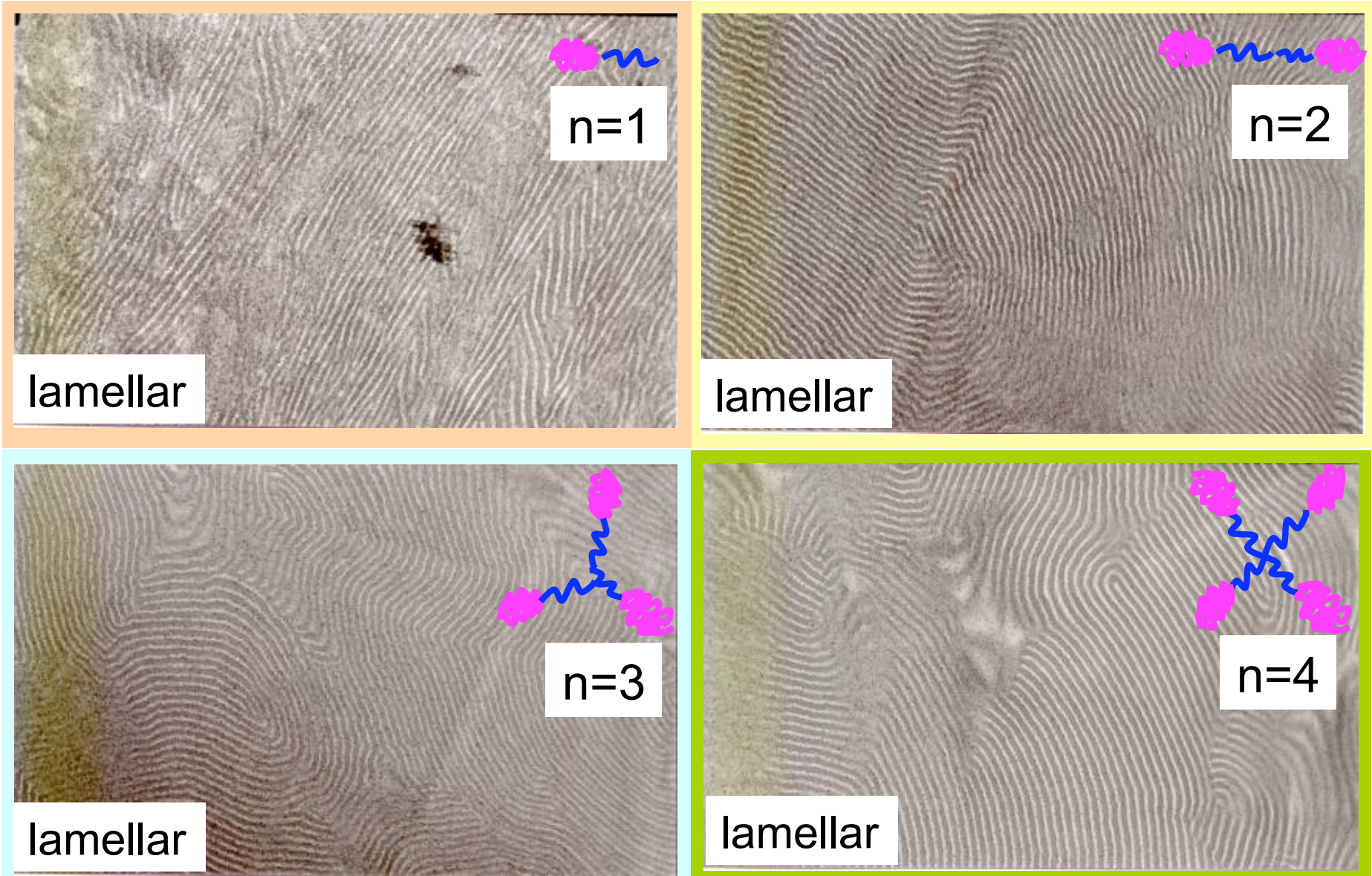


2-3 wt% anti-oxidant was melt blended at $T > T_{ODT}$
 Melt pressed at $T < T_{ODT}$ at 3MPa for 15 min.

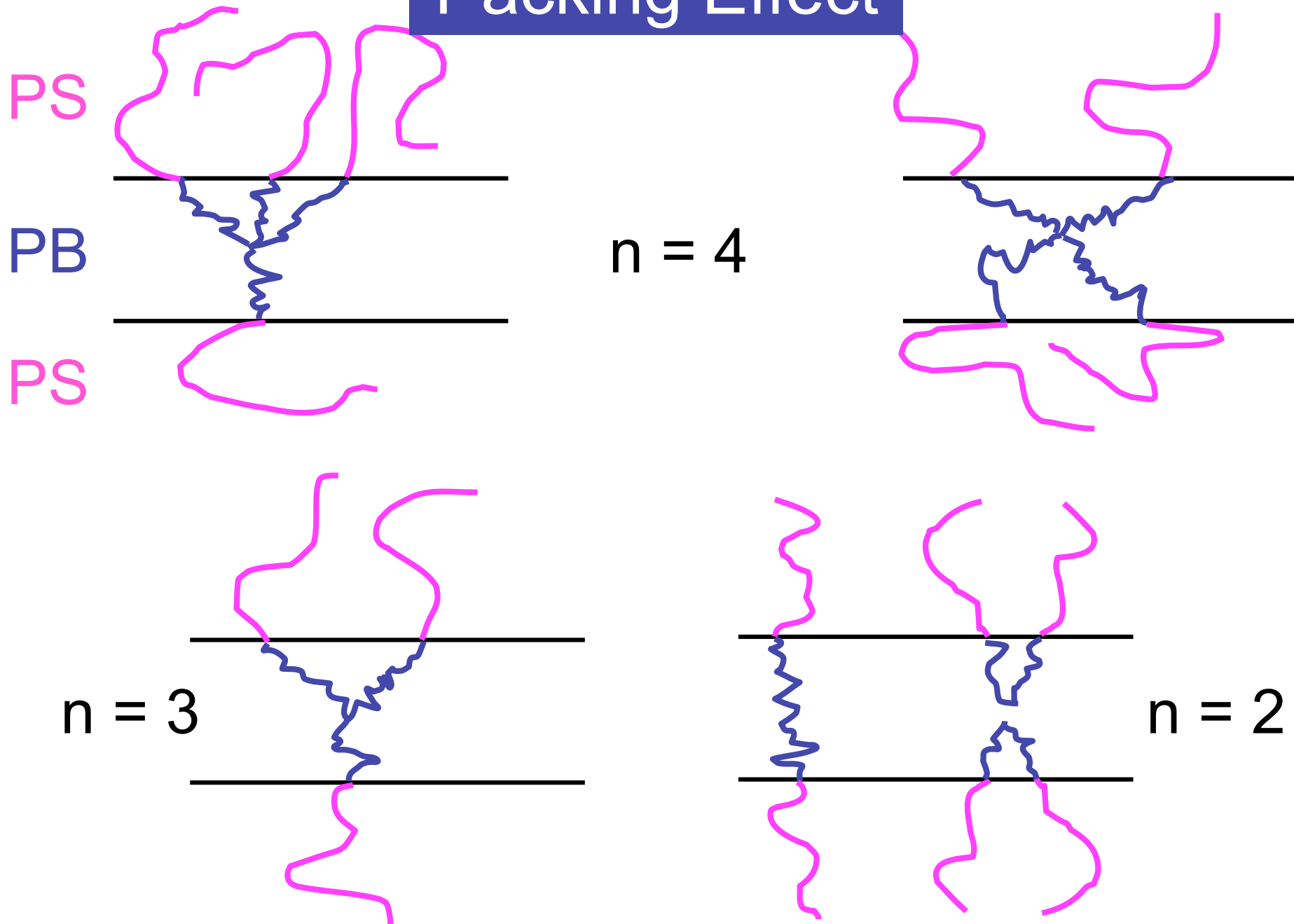
TEM Micrographs of Toluene Cast Films

Arm 10K 10K
S B

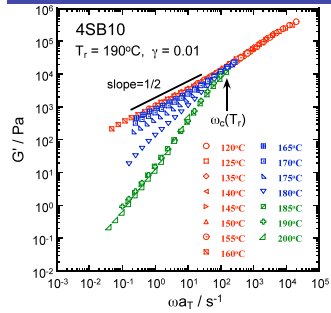
100nm



Packing Effect



Freq. Dispersion of G' for Lamellar-forming 4SB10

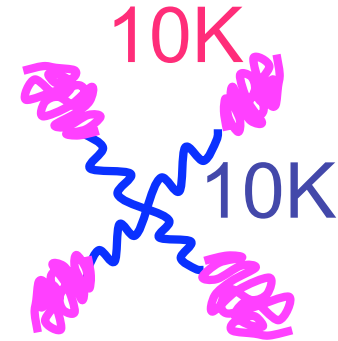


motion of lamellar domain
slope=1/2

concentration fluctuation

disordered, one phase

chain motion



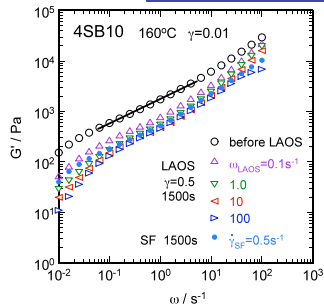
Superposition is possible in ordered and disordered states

Poly-grain states

$$G' \sim \omega^{1/2}$$

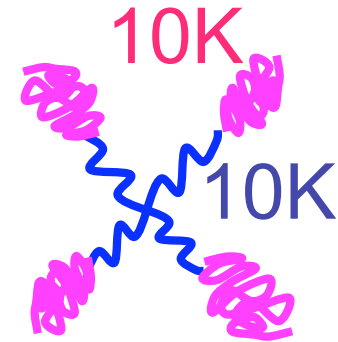
$$\text{at } \omega < \omega_C$$

Decrease in G' after LAOS for 4SB10



slope=1/2

$0.1\omega_c$



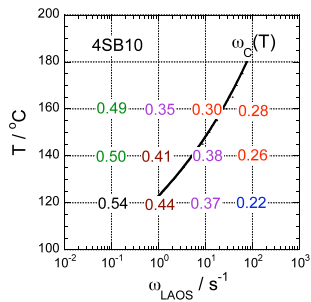
After LAOS

$\omega_{\text{LAOS}} \nearrow$ $G' \searrow$

Evaluate

$G'_{\text{after}}/G'_{\text{before}}$
at $\omega = 0.1 \omega_c$

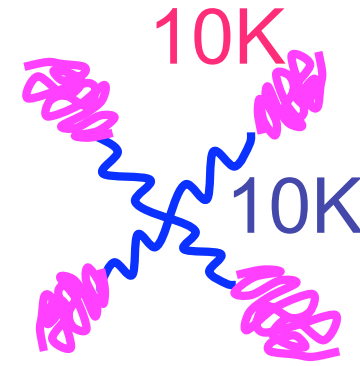
Decrease in G' after LAOS for 4SB10



(A)

(B)

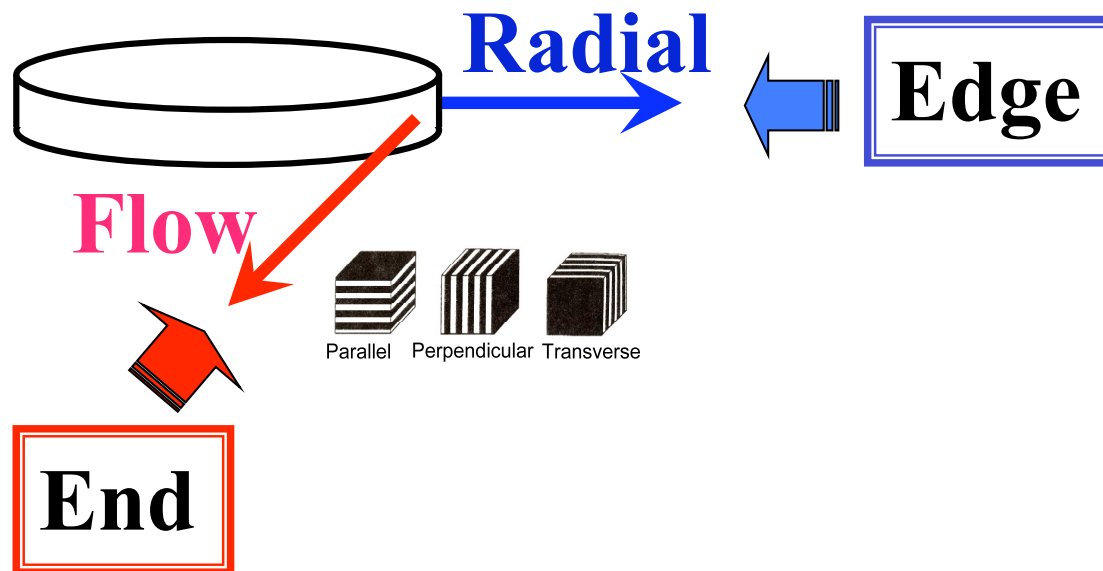
(C)



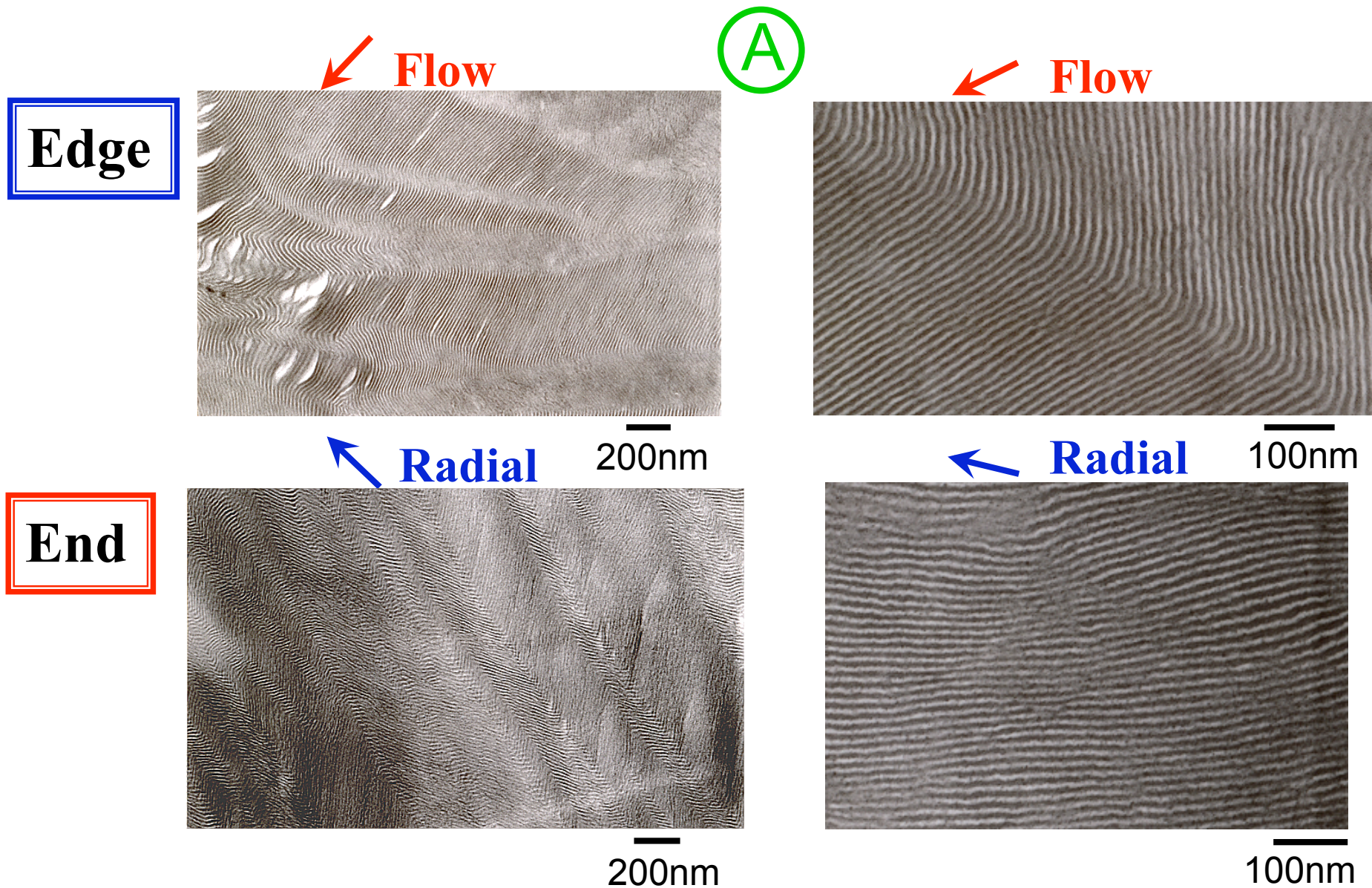
(D)

At each T
 $G'_{\text{after}}/G'_{\text{before}} \searrow$
 $\omega_{\text{LAOS}} \nearrow$

Observation of Lamellar Orientation

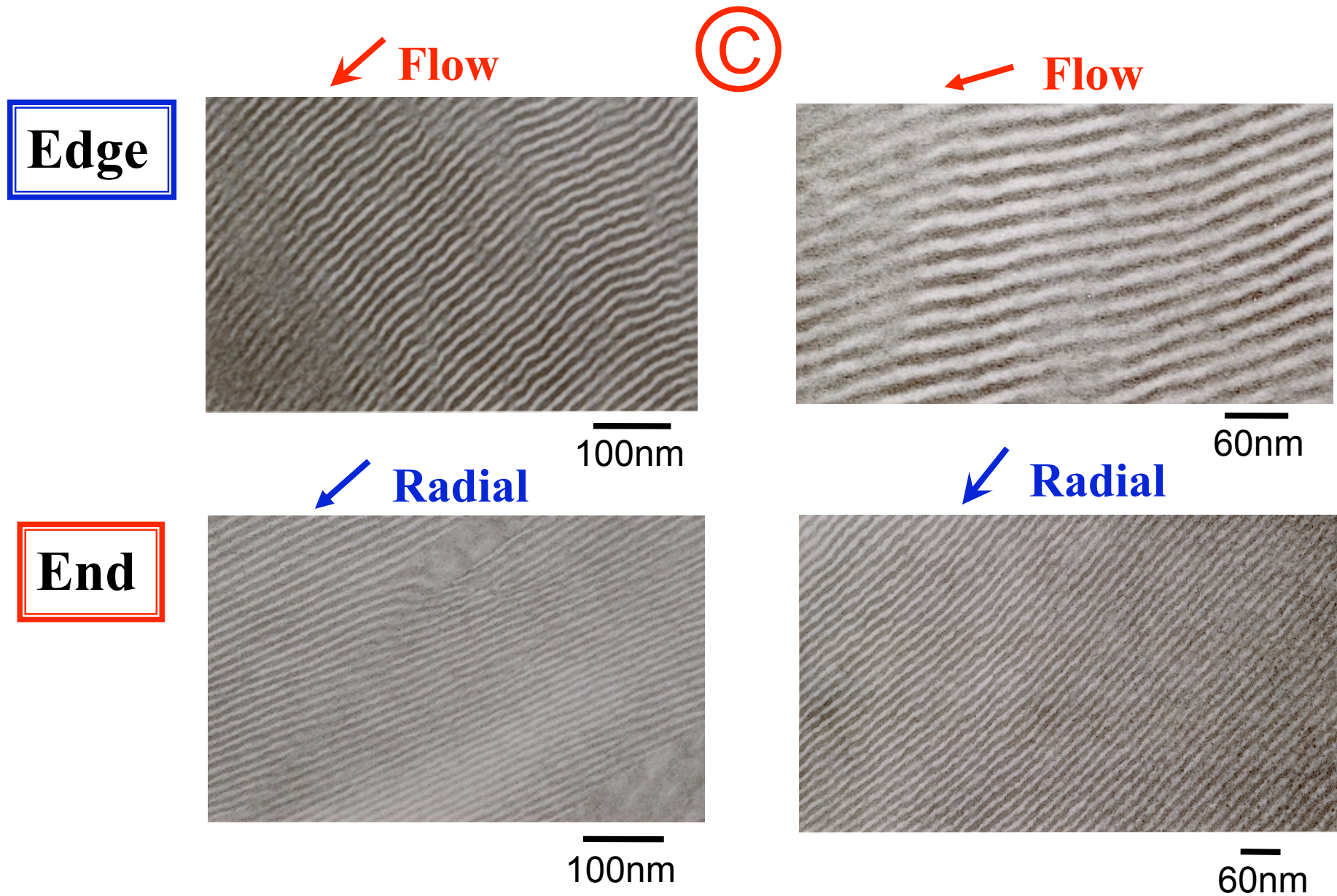


TEM Micrographs of 4SB10 after LAOS ($\omega_{\text{LAOS}}=0.1\text{s}^{-1}$, 160°C)



Parallel > Perpendicular \gg Transverse

TEM micrographs of 4SB10 after LAOS ($\omega_{\text{LAOS}}=10\text{s}^{-1}$, 160°C)

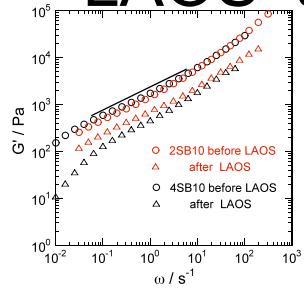


Parallel orientation is prevailing

Effect of n (=2,4) on G' Reduction

LAOS at $\gamma = 0.5$

$$\omega_{\text{LAOS}}/\omega_C \cong 0.80 \quad T/T_{\text{ODT}} \cong 0.90$$



slope=1/2

Data of 2SB10 are superposed onto those of 4SB10 at $\omega \geq \omega_C$

n=2

n=4

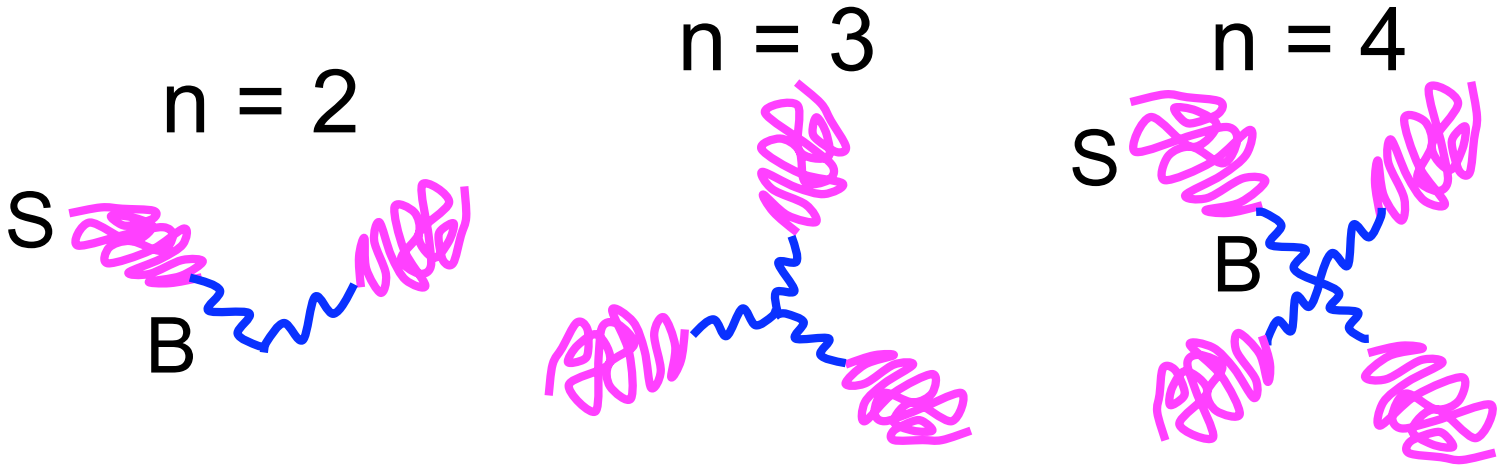
When $n \uparrow$, $G' \downarrow$ due to stronger orientation of lamellae

Cylinder-Forming
SB Starblock Copolymers

(SB)_n Star Block Copolymers

┌ Arm ─┐

n	Code	M _n (PS)	M _n (PB)	f _{PB}	
2	2SB20	20.0K	10.5K	0.34	C
3	3SB20	19.9K	10.8K	0.35	C
4	4SB20	19.9K	10.2K	0.34	C



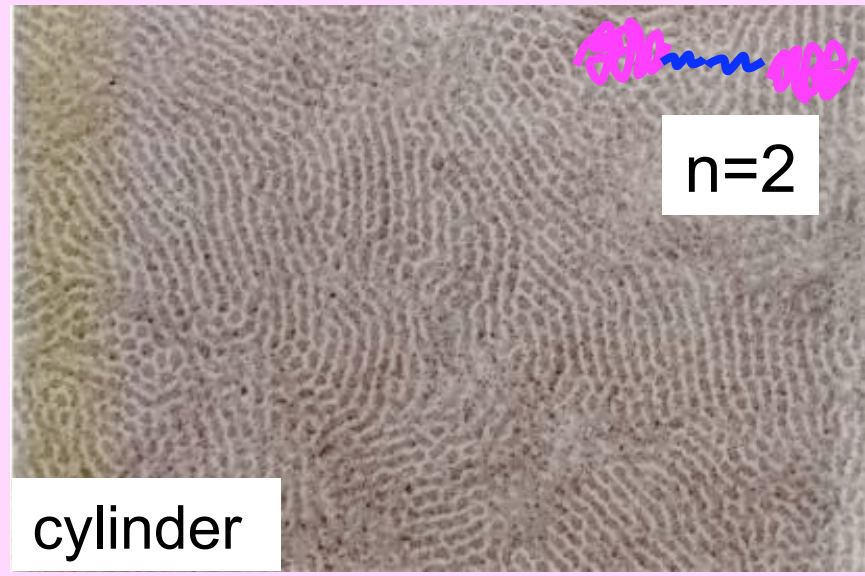
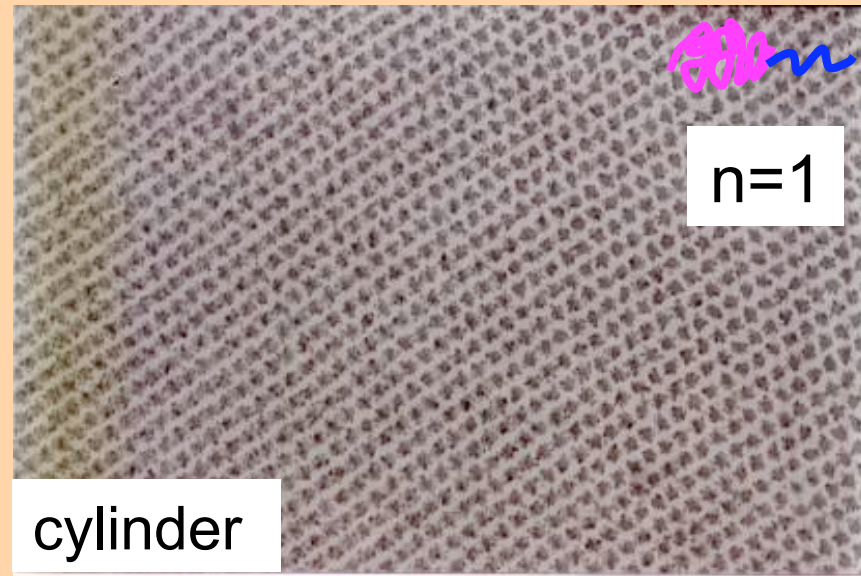
2-3 wt% anti-oxidant was melt blended at $T > T_{ODT}$
 Melt pressed at $T < T_{ODT}$ at 3MPa for 15 min.

TEM Micrographs of Toluene Cast Films

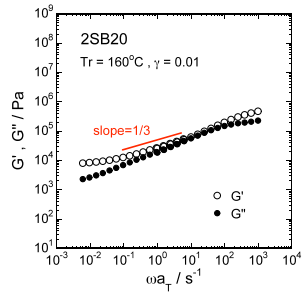
Arm

20K S
10K B

100nm



Freq. Dispersion of G' , G'' for Cylinder-forming 2SB20



20K 10K
Handwritten scribbles in pink and blue

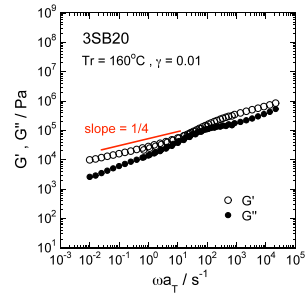
ω_C
↓

In poly-grain state

$$G' \sim \omega^{1/3}$$

at $\omega < \omega_C$

Freq. Dispersion of G' , G'' for Cylinder-forming 3SB20



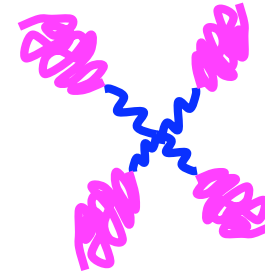
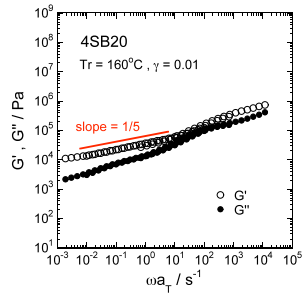
ω_C
↓

In poly-grain state

$$G' \sim \omega^{1/4}$$

at $\omega < \omega_C$

Freq. Dispersion of G' , G'' for Cylinder-forming 4SB20



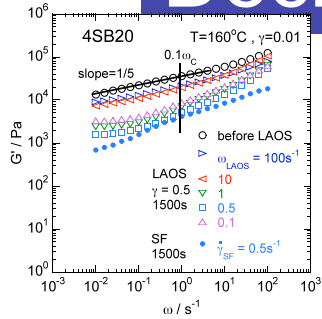
ω_C
↓

In poly-grain state

$$G' \sim \omega^{1/5}$$

at $\omega < \omega_C$

Decrease in G' after LAOS and SF for 4SB20

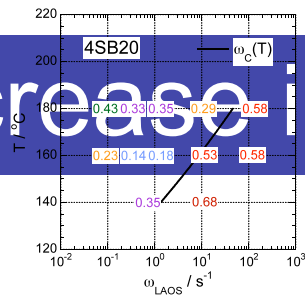


After LAOS
 G' shows
 minimum at
 $\omega_{\text{LAOS}} = 0.5\text{s}^{-1}$

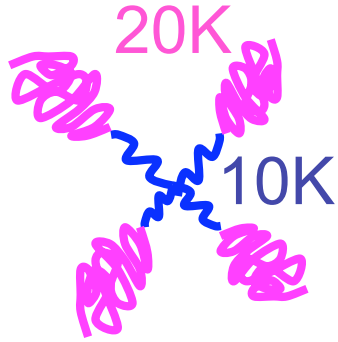
$$\omega_{\text{LAOS}} = \dot{\gamma}_{\text{SF}} = 0.5\text{s}^{-1}$$

SF is more effective
 for cylinder orientation

Decrease in G' due to LAOS

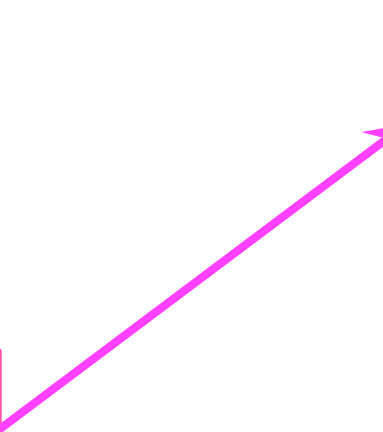
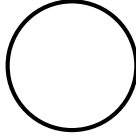
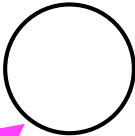


	η	f/G'
m1	226.77	1.79e+308
m2	2155.3	1.79e+308
m3	15.727	1.79e+308
f/J'C:Q	1.6156e-27	NA
R	1	NA

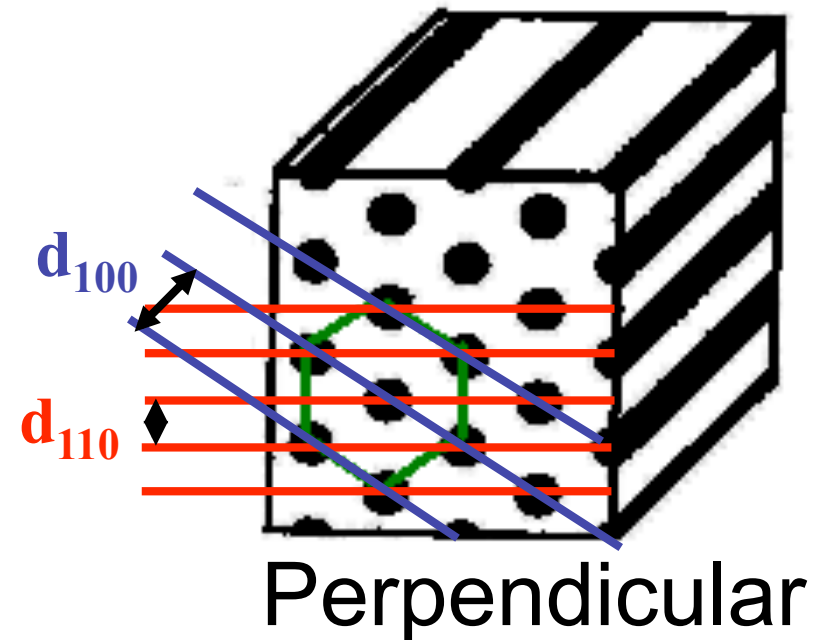
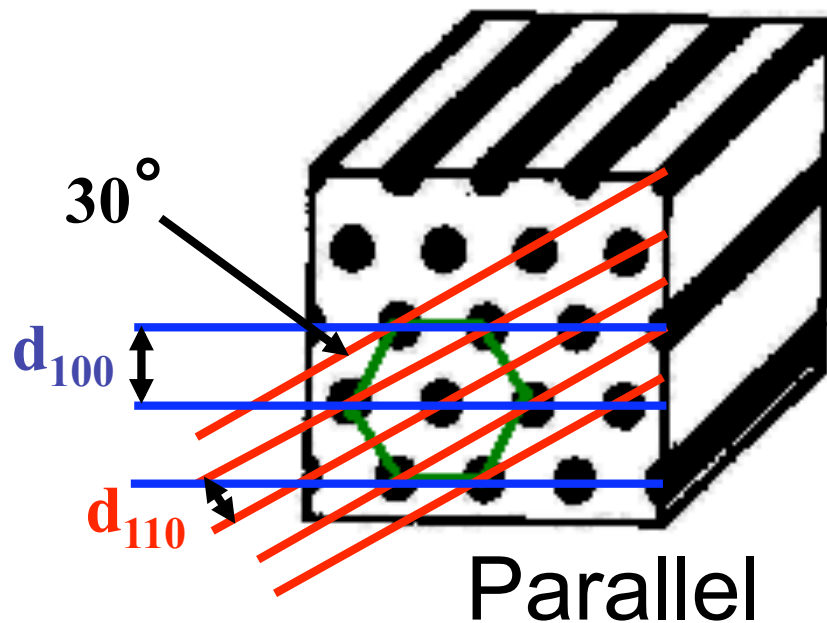
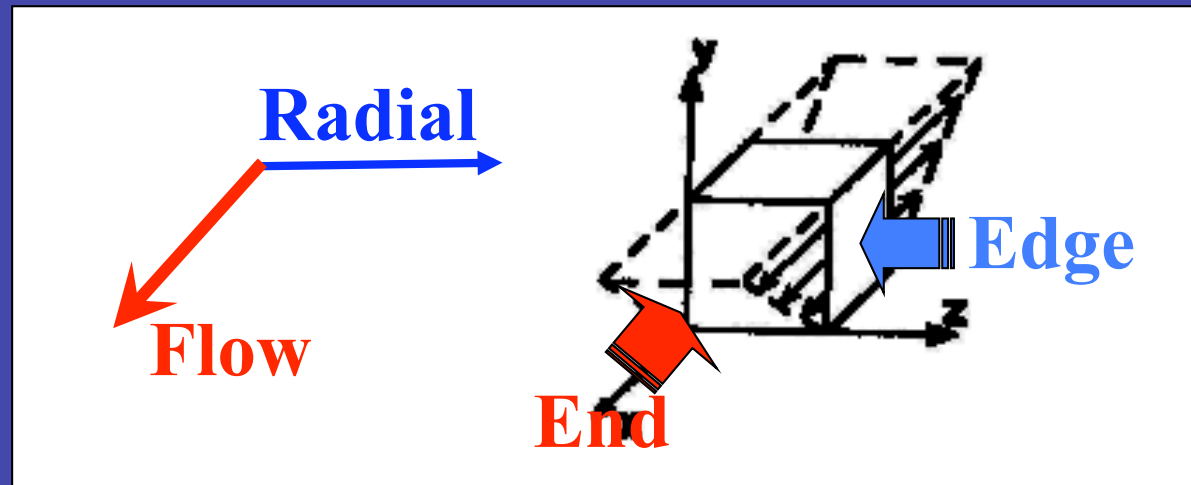


At 160°C, 180°C
 $\omega_{LAOS} \nearrow \Rightarrow G' \searrow \nearrow$

For SF
 $G'_{after} / G'_{before} = 0.10$

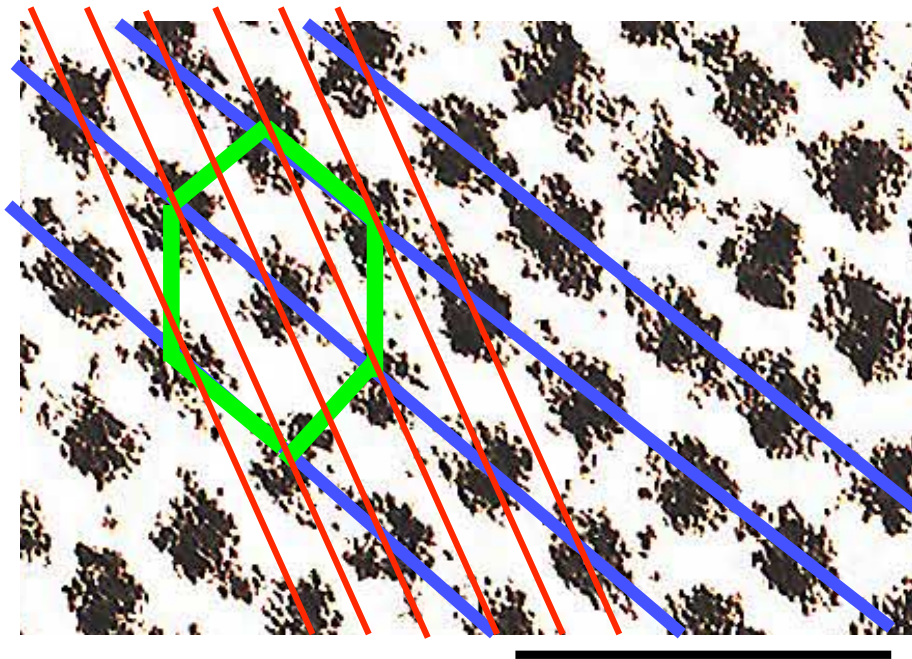


Orientation of Hexagonal Cylinders



4SB20 at $\omega_{\text{LAOS}} = \dot{\gamma}_{\text{SF}} = 0.5\text{s}^{-1}$ (160°C)

After LAOS



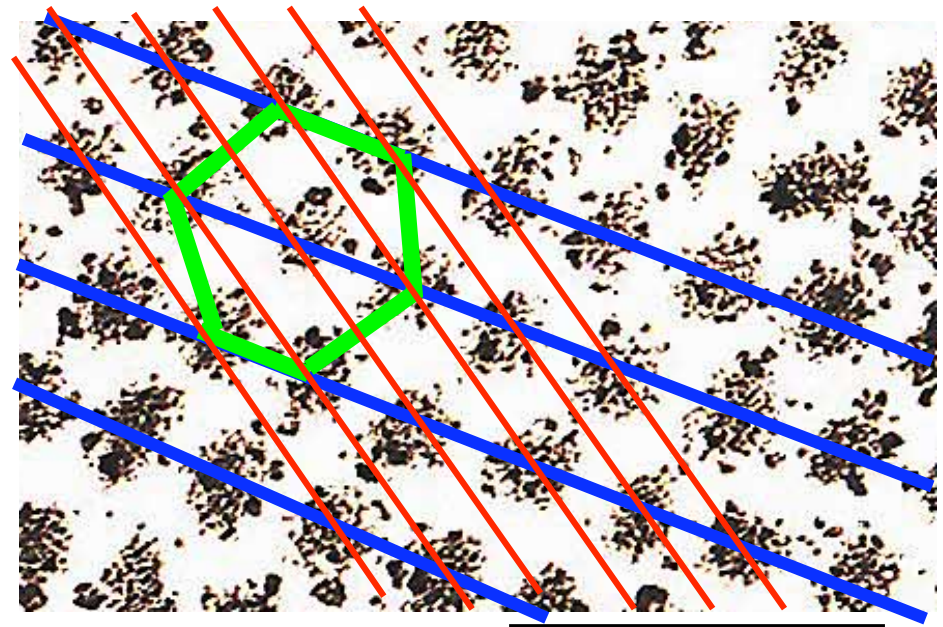
60nm

End

⊙
Flow

↙
Radial

After SF



60nm

End

⊙
Flow

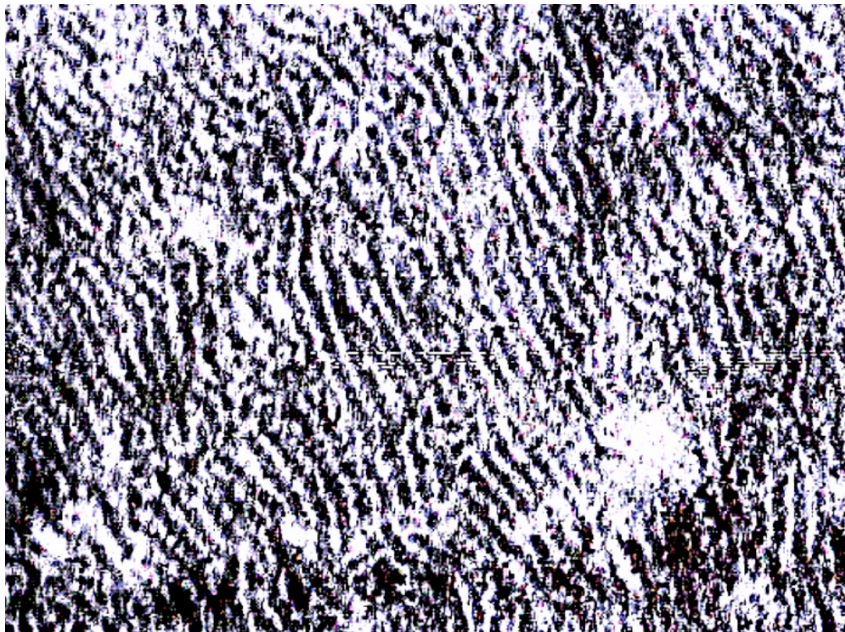
↙
Radial

SF is more effective for Parallel Orientation

4SB20 after LAOS ($\omega_{\text{LAOS}} = 100\text{s}^{-1}$, 160°C)

End

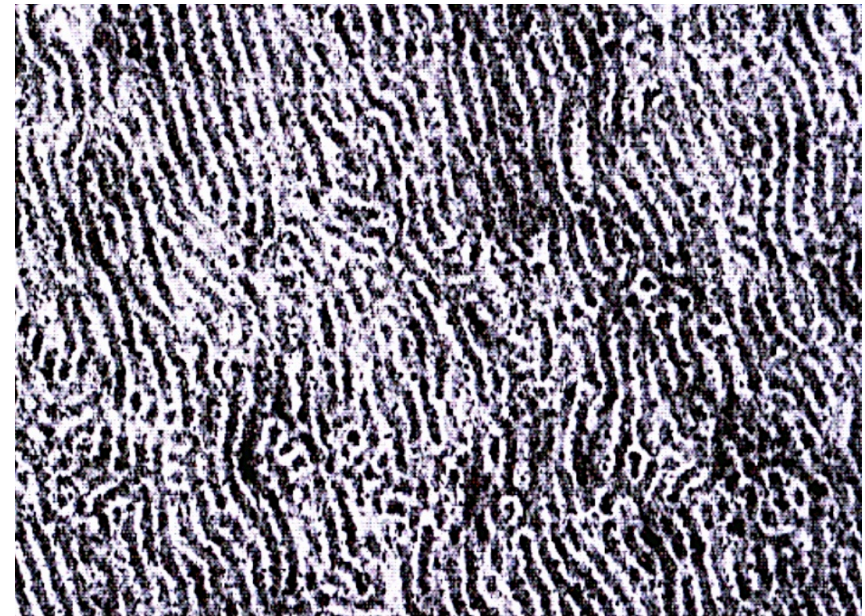
⊙ **Flow** ↙ **Radial**



100nm

Edge

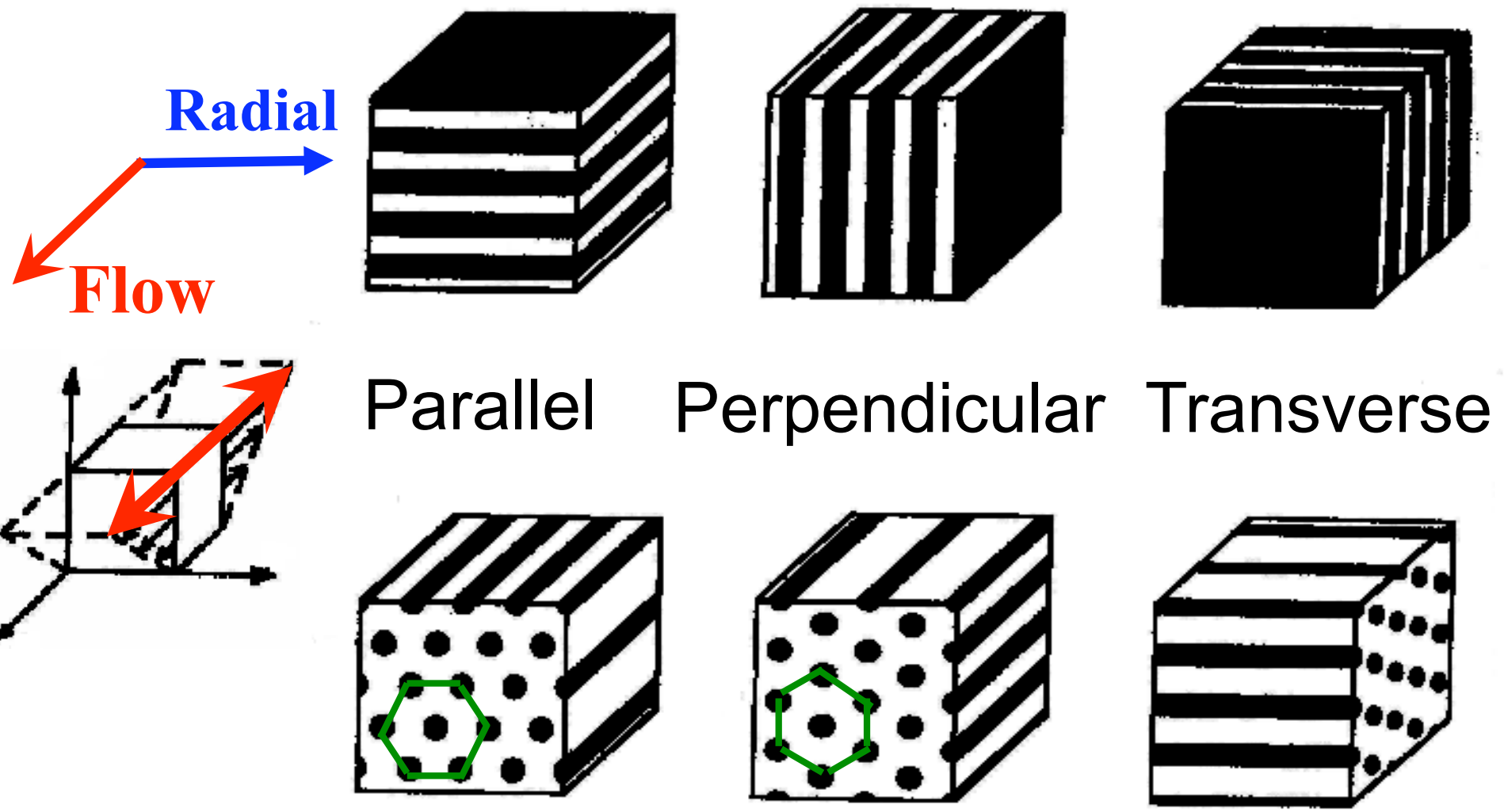
⊙ **Radial** ↙ **Flow**



100nm

Cylinders are **perpendicular** to the disc surface!!

Orientations of Lamellae and Cylinders



Conclusions

For lamellar-forming samples

- 1) In ordered state, $G' \sim \omega^{1/2}$.
- 2) After LAOS, G' decreases with **increasing** ω_{LAOS} due to parallel orientation.
- 3) Perpendicular orientation is also observed for low ω_{LAOS} .

For cylinder-forming samples

- 1) In ordered state, $G' \sim \omega^{1/(n+1)}$.
- 2) After LAOS, G' decreases with **decreasing** ω_{LAOS} (showing minimum) due to parallel orientation.
- 3) SF is more effective for parallel orientation.
- 4) For $\omega_{\text{LAOS}} > \omega_{\text{C}}$, cylinders orient perpendicular to disc.

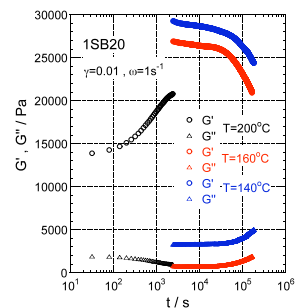
Time sweep of G' , G'' for 1SB20

20K 10K



$C \rightarrow G$ is fast

$G \rightarrow C$ is slow



G

G

C

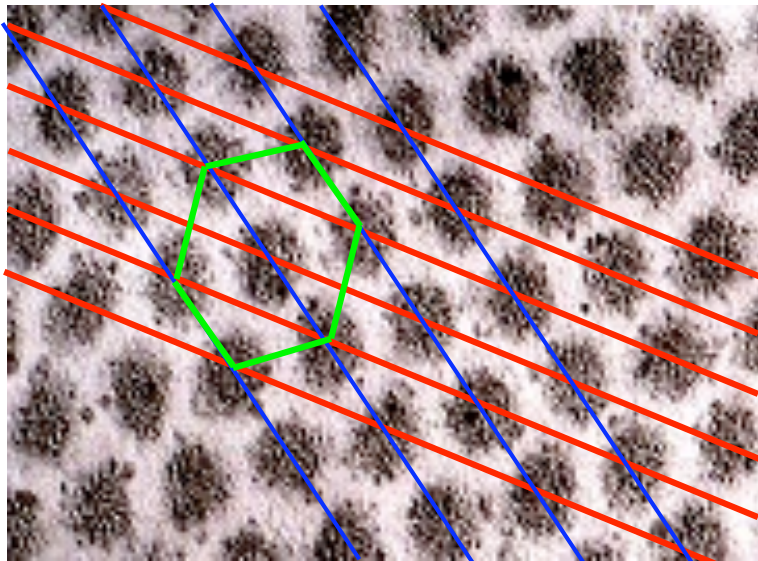
C

G'

G''

2SB20 at $\omega_{\text{LAOS}} = \dot{\gamma}_{\text{SF}} = 0.5\text{s}^{-1}$ (160°C)

After LAOS



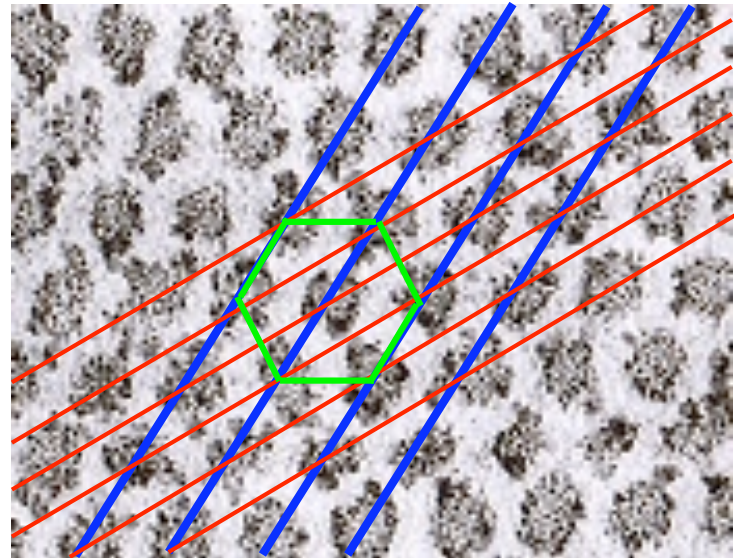
60nm

End

○
Flow ←
Radial

Perpendicular orientation

After SF



60nm

End

○
Flow ↗
Radial

Parallel orientation

Theories for Slow Relaxation behavior

Lamellar-forming, Poly-grains (randomly oriented)

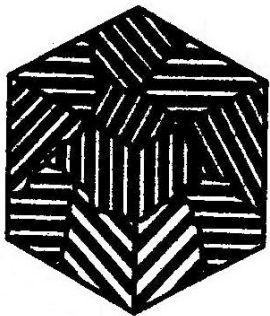
Kawasaki-Onuki (1990)

Hydrodynamic mode of lamellar motion
Overdamped second-sound mode

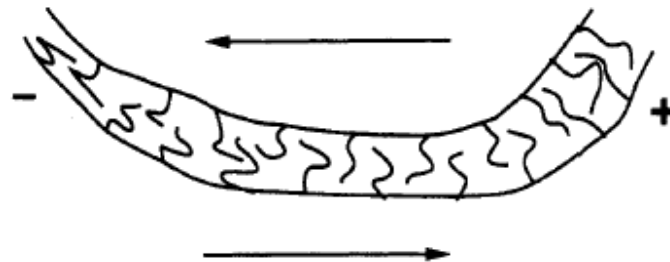
$$G'(\omega) \cong G''(\omega) \cong \frac{\pi}{24\sqrt{2}} (B\eta_0)^{1/2} \omega^{1/2}$$

B : bending modulus of lamella

η_0 : viscosity in the disordered phase



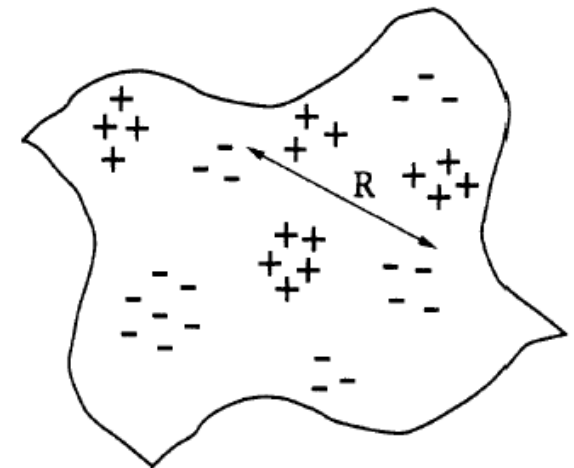
randomly oriented



Rubinstein-Obukhov (1993)

Collective diffusion of copolymer chains along the interface
controlled by defects

$$G'(\omega) \cong G''(\omega) \sim \omega^{1/2}$$



Mechanisms of lamellar orientation

1. Selective rotation of grains
2. Selective melting and reformation of lamellae
3. Defect migration
4. Reduction of mechanical resistance
5. Tube orientation (for entangled chains)
6. Coupling of the lamella motion and the shear field (shear-induced lamella formation)

H.Watanabe in “Structure and Properties of Multiphase Polymeric Materials”, pp. 317-360, Marcel Dekker, New York (1998)